

Higher order Magnus expansions for two-level quantum dynamicsChen Wei and Frank Großmann^{a)}*Institut für Theoretische Physik, Technische Universität Dresden, 01062 Dresden, Germany*

(Dated: 17 March 2026)

We investigate the Magnus expansion for a generic time-dependent two-level system under single-axis driving. By virtue of the $\mathfrak{su}(2)$ Lie algebra, the expansion is decomposed into a commutator-free form. To illustrate the usefulness of the gained expression, we then revisit the Landau-Zener-Stückelberg-Majorana model, with a focus on non-adiabatic transitions as well as the Stokes phase. In addition, the semiclassical Rabi model is systematically treated by determining the Floquet quasienergy up to different orders. We demonstrate how to employ suitable picture transformations as well as on how to enforce the symmetry of the underlying model in order to guarantee convergence of the expansion as well as to achieve satisfactory agreement with the exact results. For both models that we studied it turns out that a third order approximation yields results that are in next to perfect agreement with exact analytical ones. Surprisingly, in the case of the semiclassical Rabi model, even the second order Magnus approximation in the adiabatic picture produces almost exact results over the whole parameter range.

Keywords: Magnus expansion, quantum dynamics, two-level system, Floquet quasienergy, Landau-Zener-Stückelberg-Majorana model, Stokes phase, semiclassical Rabi model, adiabatic picture

^{a)}Electronic mail: frank.grossmann1@tu-dresden.de

I. INTRODUCTION

In this work we investigate the Magnus expansion¹ (ME) with a focus on two-level quantum dynamics under single-axis driving, modeled by the Hamilton operator

$$H(t) = \frac{\Delta}{2}\sigma_z + \frac{f(t)}{2}\sigma_x, \quad (1)$$

with Pauli matrices σ_z, σ_x and where Δ is a (positive) constant while $f(t)$ may be arbitrarily time-dependent. Hamilton operators in the form of Eq. (1) have a long tradition starting in the heyday of quantum theory, with the works of Landau, Zener, Stückelberg and Majorana (LZSM)²⁻⁵, as well as Rosen and Zener (RZ)⁶. In addition, the semiclassical Rabi model⁷⁻¹⁰ with a linearly polarized drive falls into this class. It is striking that although the quantum dynamics of LZSM and RZ models have long been known to be solvable analytically exactly, the semiclassical Rabi model has only been solved analytically without employing the rotating wave approximation in the early 21st century^{11,12}. Furthermore, alternative (as well as more insightful) derivations and interpretations of Landau-Zener transitions are published up to the present days¹³⁻¹⁸ and the relevance of the above models in different fields of physics and chemistry cannot be overemphasized. Applications are ranging from molecular collisions^{19,20} and driven quantum tunneling²¹⁻²⁷ to quantum state preparation²⁸⁻³⁰, to name but a few.

The interest in two-level quantum dynamics has persisted in recent times, driven by the increasing relevance of qubit dynamics and control^{22,31}. For the well-known exactly solvable cases mentioned above, non-elementary special functions are frequently encountered, making them impractical for applications and physical interpretation, however. In order to mitigate this problem, reverse engineering approaches have been developed^{32,33}, enabling the construction of infinitely many analytically solvable driving functions $f(t)$. However, it remains unclear how the general dynamical behavior is determined by external driving with, e.g., pulsed laser fields. For example, previous studies have observed that although the pulse shapes may be qualitatively similar, the system's evolution will depend sensitively on their precise form in the case of non-resonance of the drive³⁴⁻³⁶.

Groundbreaking efforts to understand general aspects of two-state quantum dynamics have been made, particularly in the context of non-adiabatic transitions. Based on the work of Davis and Pechukas³⁷ and Berry³⁸, non-adiabatic transitions can be understood by

analyzing the singularities of the Hamiltonian under analytic continuation into the complex-time plane. This approach yields the correct exponent for the LZ transition probability and the underlying ideas were taken up by the so-called exact WKB analysis³⁹, which has been extensively developed and discussed in the past few years. While this approach is promising, its mathematical complexity and the challenges associated with generalizing to multi-level systems limit its practical appeal. As another commonly applied approach, the Dyson series⁴⁰ converges for quantum systems with a finite-dimensional Hilbert space at any fixed time. Nevertheless, issues such as wave-function normalization and the emergence of secular terms require special care⁴¹. More fundamentally, non-perturbative effects are often exponentially small in the coupling strength and cannot be captured by any finite-order or even infinite-order perturbative expansion. A prominent example of such behavior is the so-called Landau-Zener transition in the LZSM model.

In contrast to the two approaches discussed above, the ME for the time-evolution operator exhibits an elegant simplicity. By construction, it automatically preserves the unitarity of the time-evolution operator for a Hermitian Hamiltonian, and can therefore considerably simplify the calculation. Specializing to two-level systems, the ME has been successfully applied to the Rosen-Zener problem⁴², Rashba spin-orbit coupling⁴³, Rabi models in the context of nuclear magnetic resonance^{44–46} and under chirped pulses⁴⁷ as well as to non-Hermitian two-level systems⁴⁸. Furthermore, in half-cycle pulse driven hydrogen atoms, different orders of ME have been used in different gauges to reach the same accuracy⁴⁹. As will be shown in the present paper, a low order ME approach serves as a quickly converging approximation for the LZSM problem, as well as for the semiclassical Rabi model thereby indicating its ability to describe non-perturbative effects.

Yet the ME has its own subtleties; even in the simplest case of a two-level system, it can diverge when the evolution time becomes large^{50,51}. By now, the mathematical aspects of the convergence of the ME are well-studied^{52–55}. For physical applications, on the other hand, properties of convergence can be drastically different in different pictures of quantum mechanics, as noticed by several authors^{42,52,56}. The importance of convergence studies and the usefulness of picture transformations, however, have not yet been fully exploited in previous work. In the present contribution, we will make further progress in this direction. We show that it is constructive to study different parameter regimes of the Hamiltonian Eq. (1), requiring only the qualitative features of $f(t)$ to be specified. In particular, we

prove that when $f(t)$ is a monotonic function, the ME in the adiabatic picture is ensured to converge. This also provides a quantitative characterization of the adiabatic theorem⁵⁷ in the simple case of two-level systems.

The article is structured as follows: In Sec. II we lay the foundation for the rest of the article by employing the $\mathfrak{su}(2)$ algebra to reduce the ME for the two-level problem into commutator-free form, the detailed derivation of which can be found in Appendix A. Sec. III is then devoted to the reinvestigation of the non-adiabatic problem, emphasizing the importance of the adiabatic picture. Our investigations are exemplified by the LZSM problem. In Sec. IV a novel analytic computational scheme for the Floquet quasienergy of a periodically driven two-level system is proposed, based on the ME and unitary transformations. We systematically apply the scheme to the semiclassical Rabi model. The ME is found to be a versatile tool that is even more broadly applicable as well as more powerful (quickly converging) than it might have been expected. We conclude with a discussion of the presented results and the future potential of the ME in Sec. V. Two further Appendices B and C deal with the symmetries of the problems discussed and with the different types of quasienergy crossings encountered, respectively.

II. SU(2) GROUP AND MAGNUS EXPANSION

In general, the quantum mechanical time-evolution operator $U(t, t_0)$ depends on two time arguments with a fixed initial time t_0 and the initial condition $U(t_0, t_0) = \mathbb{I}$, with \mathbb{I} denoting the identity operator. For notational convenience, we mostly drop the t_0 argument and assume that U can be written as an exponential for all times¹,

$$U(t) = \exp[-i\Omega(t)]. \quad (2)$$

Hereafter, $\Omega(t)$ is referred to as the Magnus operator.

Since the Hamiltonian in Eq. (1) is traceless, at each point of time, the corresponding time-evolution operator $U(t)$ belongs to the SU(2) group and admits the standard angle-axis parameterization⁵⁸. I.e., there exists a real-valued function $\theta(t)$ and a unit vector $\vec{n}(t)$ such that

$$\begin{aligned} U(t) &= \exp[-i\theta(t)\vec{n}(t) \cdot \vec{\sigma}] \\ &= \cos \theta \sigma_0 - i \sin \theta \vec{n} \cdot \vec{\sigma}, \end{aligned} \quad (3)$$

where $\vec{\sigma} = (\sigma_x, \sigma_y, \sigma_z)$ is a vector whose elements are the Pauli matrices. Comparing Eq. (3) with Eq. (2), the Magnus operator can be identified as

$$\Omega(t) = \theta(t)\vec{n}(t) \cdot \vec{\sigma}. \quad (4)$$

and it belongs to the $\mathfrak{su}(2)$ algebra, i.e., it can be represented by the set of traceless Hermitian 2×2 matrices.

The raising and lowering operators $\sigma_{\pm} := \frac{1}{2}(\sigma_x \pm i\sigma_y)$, together with σ_z , fulfill the commutation relations

$$[\sigma_z, \sigma_{\pm}] = \pm 2\sigma_{\pm}, \quad [\sigma_+, \sigma_-] = \sigma_z \quad (5)$$

and form a complete basis for $\mathfrak{su}(2)$. Thus $\Omega(t)$ can be decomposed as

$$\Omega(t) = A(t)\sigma_+ + A^*(t)\sigma_- + C(t)\sigma_z, \quad (6)$$

where the coefficient $A(t)$ is complex in general, while $C(t)$ has to be real-valued. Comparing Eq. (4) with Eq. (6), the angle and axis can be expressed by these coefficients as

$$\theta = \sqrt{|A|^2 + |C|^2}, \quad (7)$$

$$\vec{n} = \frac{1}{\theta}(\text{Re}(A), -\text{Im}(A), C). \quad (8)$$

The quantities in Eqs. (7,8) will be the main objects of the calculations in this work. In Appendix A, we review the derivation of the series expansion

$$A(t) = \sum_{n=1}^{\infty} A_n(t), \quad C(t) = \sum_{n=1}^{\infty} C_n(t) \quad (9)$$

and the recursion relations for $A_n(t)$ and $C_n(t)$. Later-on, we refer to them as the Magnus coefficients (MC). Up to this point, our discussion is valid for the most general two-level Hermitian Hamiltonian.

While a Hamiltonian in the form of Eq. (1) admits for a direct physical interpretation, for reasons that will become clear later, we will switch to a Hamiltonian of the form

$$H(t) = v(t)\sigma_+ + v^*(t)\sigma_-, \quad (10)$$

where $v(t)$ is a complex scalar function, which can be expressed by $f(t)$ and Δ in different ways for different pictures of quantum mechanics, see for example Eq. (27) and Table I further below. For a Hamiltonian in the above special form, by using Eq. (A15) and Eq. (A12), it can be recursively verified that

$$A_{2n}(t) = C_{2n-1}(t) = 0, \quad \forall n \geq 1, \quad (11)$$

i.e., all even indexed A -coefficients and all odd-indexed C -coefficients vanish, considerably simplifying our efforts. Defining $v_1 := v(t_1), v_2 := v(t_2) \dots$, the three leading non-zero coefficients read

$$A_1(t) = \int_0^t dt_1 v_1, \quad (12)$$

$$C_2(t) = \int_0^t dt_1 \int_0^{t_1} dt_2 \operatorname{Im}[v_1 v_2^*], \quad (13)$$

$$A_3(t) = \frac{2i}{3} \int_0^t dt_1 \int_0^{t_1} dt_2 \int_0^{t_2} dt_3 \left[\operatorname{Im}(v_2 v_3^*) v_1 + \operatorname{Im}(v_2 v_1^*) v_3 \right]. \quad (14)$$

Commutator free equations for the coefficients similar to the ones above have been found before directly from the ME⁴⁸, while in Appendix A we employ the $\mathfrak{su}(2)$ decomposition to provide a systematic treatment. For the use of related commutator-free time-evolution operators in numerical applications, we refer to⁵⁹.

According to Maricq⁵², a sufficient convergence condition for the two-level system ME is given by

$$\int_{t_0}^t E(s) ds < \pi, \quad (15)$$

where $E(t)$ is the positive instantaneous eigenvalue of the Hamiltonian. In the case of Eq. (10), we have

$$E(t) = |v(t)|. \quad (16)$$

We note that $E(t)$ can be regarded as the operator norm of a 2×2 traceless Hermitian matrix, and therefore Eq. (15) is a special case of Casas' π -criterion⁵⁵ for general bounded Hamiltonians. The different performance of the ME in different pictures of quantum mechanics can be traced back to the fact that the norm of the Hamiltonian may differ drastically by switching to another picture as will be seen in Section IV.

III. NON-ADIABATIC TRANSITION PROBLEM

The (quantum) adiabatic theorem states that a quantum system initially prepared in an instantaneous eigenstate of an infinitely slowly varying Hamiltonian remains in the corresponding instantaneous eigenstate throughout the evolution, up to a phase factor^{57,60}. The non-adiabatic transition problem deals with the determination of transition probabilities between instantaneous eigenstates of a time-dependent Hamiltonian when the adiabatic

condition is violated. This problem can be most cleanly addressed in the adiabatic (interaction) picture^{42,61,62}, as reviewed below. We note that the ME in the adiabatic picture has been paid special attention to in previous works, such as^{42,63}. In the following we point out that the convergence condition Eq. (15), which has this far not been in the center of interest, holds for a large class of drivings.

A. Adiabatic picture

To start with, we choose the instantaneous eigenstates of the Hamiltonian of Eq. (1) under the real-gauge^{38,64}

$$|\phi_+(t)\rangle = \begin{bmatrix} \cos[\chi(t)/2] \\ \sin[\chi(t)/2] \end{bmatrix}, \quad (17)$$

$$|\phi_-(t)\rangle = \begin{bmatrix} -\sin[\chi(t)/2] \\ \cos[\chi(t)/2] \end{bmatrix}, \quad (18)$$

where

$$\chi(t) := \arctan[f(t)/\Delta]. \quad (19)$$

In addition, one defines the dynamical phase

$$\varphi(t) := \int_{t_0}^t E(\tau) d\tau = \frac{1}{2} \int_{t_0}^t \sqrt{\Delta^2 + f^2(\tau)} d\tau, \quad (20)$$

where $E(t)$ is the positive instantaneous eigenvalue of the Hamiltonian of Eq. (1) and the lower limit of integration t_0 can be chosen arbitrarily.

The adiabatic picture then follows by expanding the wave function in instantaneous eigenstates, according to

$$|\psi(t)\rangle = \alpha(t)e^{-i\varphi(t)}|\phi_+(t)\rangle + \beta(t)e^{+i\varphi(t)}|\phi_-(t)\rangle. \quad (21)$$

This is equivalent to the unitary transformation

$$\begin{aligned} U(t) &= U_0(t)U_a(t)U_0^\dagger(t_0) \\ &= \Psi(t)\Phi(t)U_a(t)\Psi^\dagger(t_0), \end{aligned} \quad (22)$$

with $U_0(t) = \Psi(t)\Phi(t)$, where

$$\Psi(t) = [|\phi_+(t)\rangle, |\phi_-(t)\rangle], \quad (23)$$

$$\Phi(t) = \exp[-i\varphi(t)\sigma_z], \quad (24)$$

and

$$U_a(t) = \begin{bmatrix} \alpha(t) & -\beta^*(t) \\ \beta(t) & \alpha^*(t) \end{bmatrix} \quad (25)$$

denoting the time-evolution operator in the adiabatic picture.

It is clear from Eq. (19) that $\chi(t)$ does not increase beyond 2π whenever $f(t)$ evolves continuously. Thus the Berry phase⁶⁵ vanishes in our case since

$$\langle \dot{\phi}_+(t) | \phi_+(t) \rangle = \langle \dot{\phi}_-(t) | \phi_-(t) \rangle = 0. \quad (26)$$

Then according to Eq. (22) and the Schrödinger equation, one finds the Hamiltonian for $U_a(t)$ to be given by

$$\begin{aligned} H_a(t) &= -i\Phi^\dagger(t)\Psi^\dagger(t)\dot{\Psi}(t)\Phi(t) \\ &= \frac{\dot{\chi}(t)}{2} \begin{bmatrix} 0 & ie^{2i\varphi(t)} \\ -ie^{-2i\varphi(t)} & 0 \end{bmatrix}. \end{aligned} \quad (27)$$

Note that Eq. (27) is in accord with the structure of the Hamiltonian in Eq. (10) with the identification

$$v(t) = i\frac{\dot{\chi}(t)}{2}e^{2i\varphi(t)}, \quad (28)$$

$$\dot{\chi}(t) = \frac{\Delta\dot{f}(t)}{\Delta^2 + f^2(t)}. \quad (29)$$

Remarkably, in the time interval where $f(t)$ is monotonic, the convergence condition Eq. (15) is always satisfied. To see this, we first assume that $f(t)$ monotonically increases on $t \in [t_0, t_1]$, and hence $\dot{f}(t) > 0$. Then according to Eq. (28), the instantaneous positive eigenvalue reads

$$E(t) = |v(t)| = \frac{\dot{\chi}(t)}{2} \quad (30)$$

and hence by using the definition in Eq. (19), we find

$$\int_{t_0}^{t_1} E(\tau)d\tau = \frac{1}{2}[\chi(t_1) - \chi(t_0)] \leq \frac{\pi}{2} < \pi. \quad (31)$$

One may draw the same conclusion if $f(t)$ is monotonically decreasing instead.

Furthermore, it can be seen from Eq. (31) that Eq. (15) holds also for a bell-shaped driving. Indeed, assuming that $f(t)$ is peaked at the origin and decays monotonically away from $t = 0$, by splitting the integration interval in two pieces, we find

$$\begin{aligned} \int_{-\infty}^t E(\tau)d\tau &\leq \frac{1}{2}|\chi(-\infty) - \chi(0)| + \frac{1}{2}|\chi(0) - \chi(t)| \\ &< \pi. \end{aligned} \quad (32)$$

Thus, the Magnus expansion can be safely applied to the non-adiabatic transition problem for a large class of drivings. For example, the LZSM driving $f(t) = vt$ is monotonic over the whole time domain, while the Rosen-Zener^{6,42} driving $f(t) \propto \text{sech}(t)$ belongs to the bell-shape type. When the driving function oscillates, the Magnus expansion can be still applied in a piecewise manner to successive time intervals.

Once the MC are determined, using Eq. (3), their equivalence to Eq. (25) is established by the relations

$$\alpha = \cos \theta - i \frac{\sin \theta}{\theta} C, \quad (33)$$

$$\beta = -i \frac{\sin \theta}{\theta} A^*, \quad (34)$$

where θ is given in Eq. (7). The non-adiabatic transition probability then follows from

$$P(t) \equiv |\beta(t)|^2 = \left| \frac{\sin \theta}{\theta} \right|^2 |A(t)|^2. \quad (35)$$

To provide an intuition for this procedure, we briefly consider the leading order approximation for the general case with the initial time $t_0 = -\infty$. By substituting Eq. (28) into Eq. (12), we get

$$A_1(t) = i \int_{-\infty}^t \dot{\chi}(s) e^{2i\varphi(s)} ds. \quad (36)$$

Meanwhile, in first-order Magnus approximation (FMA),

$$A(t) = A_1(t), \quad C(t) = 0 \Rightarrow \theta(t) = |A_1(t)| \quad (37)$$

and thus Eqs. (33),(34) turn into

$$\alpha^{\text{FMA}}(t) = \cos |A_1(t)|. \quad (38)$$

$$\beta^{\text{FMA}}(t) = -i \frac{\sin |A_1(t)|}{|A_1(t)|} A_1^*(t), \quad (39)$$

In the adiabatic limit, i.e., $|A_1(t)| \rightarrow 0$, Eq. (39) can be further approximated by

$$\beta^{\text{FMA}}(t) \approx -i A_1^*(t) = - \int_{-\infty}^t \dot{\chi}(s) e^{-2i\varphi(s)} ds, \quad (40)$$

which is also the starting point of the complex WKB approximation³⁷.

Finally, we stress that Eq. (38) contains no phase information about $\alpha(t)$. In particular, the Stokes phase^{66,67}, defined as

$$\varphi_S := -\arg[\alpha(+\infty)], \quad (41)$$

is crucial for the discussion of Landau–Zener–Stückelberg interference^{67,68}, however. We show below that φ_S can be extracted from the second (and higher) order Magnus expansion.

B. Magnus expansion for the LZSM model

As an illustrative example for its quick convergence, we now explicitly consider the Magnus expansion for the LZSM model, i.e., a linear drive of the form $f = vt$ with sweep velocity $v > 0$. Its final non-adiabatic transition probability is given exactly analytically by the so-called Landau-Zener formula^{2,3}

$$P(+\infty) = \exp(-2\pi\gamma), \quad (42)$$

with the definition

$$\gamma := \frac{\Delta^2}{4v}. \quad (43)$$

For small sweep velocities the above probability vanishes, which is a special case of a well-known general result⁶⁹. Furthermore, the Stokes phase reads

$$\varphi_S = \frac{\pi}{4} + \gamma(\ln \gamma - 1) + \arg[\Gamma(1 - i\gamma)]. \quad (44)$$

These exact results can, e.g., be found by converting the Schrödinger equation into a second-order ordinary differential equation and identifying the asymptotic behavior of its solution in terms of special functions.^{3,67}

We note that the LZSM model displays parity time-inversion (PT) symmetry, i.e., due to the fact that $f(-t) = -f(t) \in \mathbb{R}$, it follows that

$$PH^*(-t)P = H(t), \quad (45)$$

where $P = \sigma_z$. To explicitly maintain this symmetry for $H_a(t)$ in the adiabatic picture, we choose $\varphi(0) = 0$ for the dynamical phase defined in Eq. (20). Under such a choice, we find

$$PH_a^*(-t)P = H_a(t). \quad (46)$$

As shown in Appendix B, due to the PT symmetry, $A_n^*(t_f = \infty) = -A_n(t_f = \infty)$ holds for each order of the ME, i.e., the A -coefficients at infinity are purely imaginary. Furthermore, the dynamical phase in the LZSM case reads

$$\varphi(t) = \frac{1}{2} \int_0^t \sqrt{\Delta^2 + v^2 s^2} ds = \gamma g(vt/\Delta), \quad (47)$$

where $g(x) := x\sqrt{1+x^2} + \ln|x+\sqrt{1+x^2}|$ is an auxiliary dimensionless function. In addition, from Eq. (29), we find

$$\dot{\chi}(t) = \frac{v}{\Delta} \frac{1}{1 + (vt/\Delta)^2} \quad (48)$$

in the LZSM case. For convenience, we employ a dimensionless time variable $x \equiv vt/\Delta$, so that the complex function in Eq. (10) can be written as (also in dimensionless form)

$$v(x) = \frac{ie^{i2\gamma g(x)}}{2(1+x^2)}. \quad (49)$$

In FMA we now finally have

$$A_1(+\infty) = iJ, \quad (50)$$

where J is determined by taking the limit $t = +\infty$ in Eq. (36) and it can be simplified as

$$J(\gamma) = \int_0^{+\infty} \frac{\cos[\gamma(\sinh(2s) + 2s)]}{\cosh(s)} ds. \quad (51)$$

As shown in panel (a) of Fig. 1, the FMA yields qualitatively good results for the transition probability calculated from Eq. (35) together with Eq. (39). In order to uncover the Stokes phase, we have to consider at least the second order Magnus approximation (SMA), however. It then follows from the resolution for the angle of the transcendental equation

$$\tan(\varphi_S^{\text{SMA}}) = \frac{\tan \sqrt{|A_1|^2 + |C_2|^2}}{\sqrt{|A_1|^2 + |C_2|^2}} C_2, \quad (52)$$

where

$$C_2(\gamma) = \iint_{x_2 < x_1} \frac{\sin(2\gamma[g(x_1) - g(x_2)])}{(1+x_1^2)(1+x_2^2)} dx_1 dx_2. \quad (53)$$

according to Eq. (13).

For a graphical display of the results, in a final step, the integrals in Eqs. (51) and (53) and analogous expressions for higher order have to be performed numerically. The corresponding "semi-analytical" results up to third order for the transition probability as well as the Stokes phase are depicted in Fig. 1. Remarkably, the third order approximation already yields almost exact values for the transition probability over the whole range of γ that is displayed and a little less accurate results for the Stokes phase. Furthermore, when γ is either large or small, also the lower ME orders are quite accurate, i.e., we do not encounter the celebrated $\pi/3$ -problem that appears if the integration in Eq. (40) is done analytically in the complex plane in first order³⁷. The former case can be understood by noticing that the integrand in Eq. (13) oscillates faster as γ increases, and thus higher order Magnus terms vanish. While when γ is small, $H_a(t)$ varies slowly with time and thus commutators of it at different times are small. In the sudden limit $\gamma \rightarrow 0^+$, $A_1(\gamma)$ and $C_2(\gamma)$ yield the exact value $\varphi_S = \pi/4$.

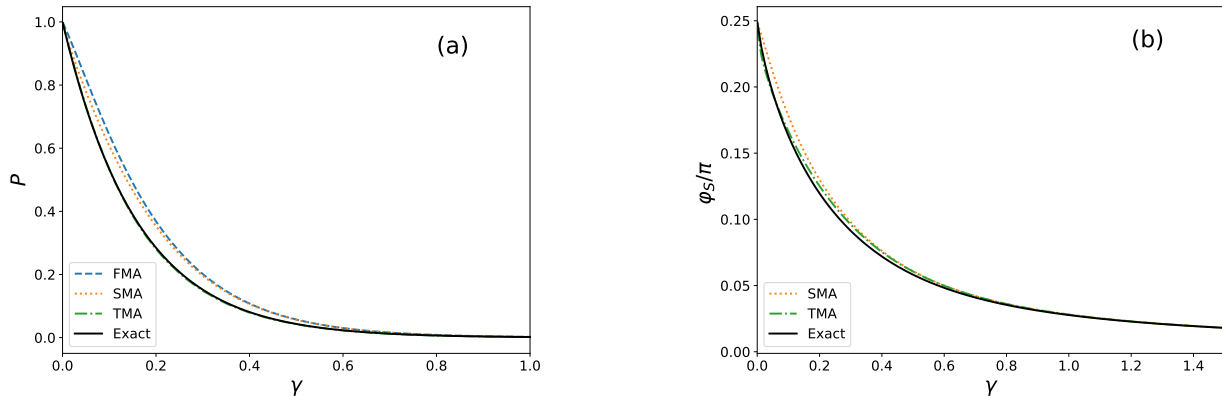


FIG. 1: Magnus approximations of different order (1st order: dashed blue, 2nd order: dotted orange, 3rd order: dash-dotted green) and exact results (solid black) for the LZSM problem: (a) transition probabilities (exact and 3rd order results are almost indistinguishable), (b) Stokes phase (1st order not shown, as it gives a zero result) in units of π , both as a function of γ , defined in Eq. (43).

IV. FLOQUET QUASIENERGIES AND THE RABI MODEL

For a time-periodic Hamiltonian with period T , the Floquet quasienergy⁷⁰ ϵ is given by the phase of an eigenvalue of the time-evolution operator over one period, $U(T)$, independent of the choice of initial time t_0 . Alternatively, the quasienergy corresponds to an eigenvalue of the effective Hamiltonian, which is defined modulo $2\pi/T$,

$$H_{\text{eff}} \equiv \frac{1}{T}\Omega(T). \quad (54)$$

The quasienergy is a conserved quantity that characterizes the system's dynamics. First applications of the Magnus approximation to periodically driven quantum dynamics have been reported in the field of nuclear magnetic resonance^{44–46}. Despite the fact that the connection between the quasienergy and the Magnus operator appears quite natural, and the so-called Floquet-Magnus expansion^{42,71} has been discussed and employed to compute H_{eff} , only few authors have used the above connection to compute the quasienergy spectrum⁴³. In this section we address the problem of calculating the quasienergies using suitable picture transformations and are refraining from using rotating frames, which corresponds to an unfavorable high frequency limit.

For a two-level system in the form of Eq. (1), in his seminal work, Shirley⁷⁰ applied the

Floquet formalism to prove the following result for the time-averaged transition probability:

$$\bar{P}_{1 \rightarrow 2} = \frac{1}{2} \left[1 - 4 \left(\frac{\partial \epsilon}{\partial \Delta} \right)^2 \right]. \quad (55)$$

This Hellmann-Feynman like result allows us to directly gain a physical understanding from the quasienergy spectrum as a function of Δ . For example, the resonance condition is located at avoided crossings since $\frac{\partial \epsilon}{\partial \Delta} = 0$. At exact crossings, however, transition probabilities may become zero²¹

A more detailed discussion of quasienergy crossings is provided in Appendix C. Technically, however, to distinguish exact and avoided crossings poses a subtle problem: although a two-level system can be easily integrated numerically, the gap of the avoided crossing could be so small that it is buried in numerical errors. One of our goals in this section is to show that using the ME, which allows analytical approximations, the two kinds of crossings can be correctly identified.

A. Quasienergy computation via Magnus expansion

For a periodically driven two-state system there is only one independent quasienergy which can be determined from the rotation angle $\theta(t)$ in Eq. (3) via

$$\epsilon = \frac{\theta(T)}{T} = \frac{\theta(T)}{2\pi} \omega, \quad (56)$$

where $\omega = 2\pi/T$ is the driving frequency.

To isolate the effect of the driving strength, we rewrite the function $f(t)$ in Eq. (1) as

$$f(t) \equiv g \tilde{f}(t), \quad g > 0, \quad \tilde{f}(t+T) = \tilde{f}(t), \quad |\tilde{f}(t)| \leq 1,$$

where g denotes the driving strength and thus the shape function $\tilde{f}(t)$ is dimensionless. With $\tilde{f}(t)$ given, there are only two independent dimensionless parameters, which can be chosen as g/ω and Δ/ω . For notational convenience, in the following we choose $\omega = 1$ and thus $T = 2\pi$. To recover the dimension, one uses the correspondence

$$\epsilon = \epsilon \left(\frac{\Delta}{\omega}, \frac{g}{\omega} \right) \omega. \quad (57)$$

Our strategy to compute the quasienergy is as follows: we divide the entire (g, Δ) plane into three parameter regimes as indicated in Fig. 2 and employ suitable picture transforms

	I: $g < \omega$	II: $\Delta < \omega$	III: $g > \omega, \Delta > \omega$
$v(t)$	$\frac{g}{2}\tilde{f}(t)e^{-i\Delta t}$	$\frac{\Delta}{2}e^{iF(t)}$	$\frac{1}{2}\dot{\chi}(t)e^{-i2\varphi(t)}$

TABLE I: Parameter regimes and the corresponding functions $v(t)$ that enter the interaction picture version of Eq. (10), which is employed for computing the Floquet quasienergy via the Magnus expansion.

such that the ME can be safely applied. Our scheme is summarized in Table I, where $v(t)$ is the crucial ingredient for the Hamiltonian. For each parameter region, $v(t)$ is chosen such that the instantaneous energy $E(t) \equiv |v(t)|$, corresponding to the operator norm, is small so that the ME exhibits controllable convergence properties.

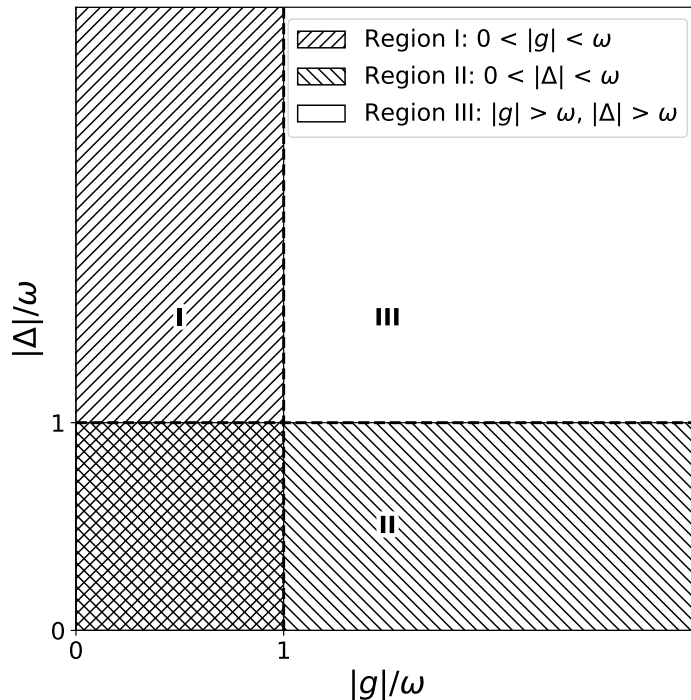


FIG. 2: Parameter regions for which the Floquet quasienergies of the semiclassical Rabi model are investigated.

Region I: $|g| < \omega$

Let us first consider the case $|g| < 1 = \omega$, where we regard the off-diagonal part of Eq. (1) as the perturbation and transform into the corresponding interaction picture. More specifically, we let $H(t) = H_0 + V(t)$ with

$$H_0 = \frac{\Delta}{2}\sigma_z, \quad V(t) = \frac{g\tilde{f}(t)}{2}\sigma_x. \quad (58)$$

For the transformation into the interaction picture, we use the unitary transformation

$$U_0(t) = \exp\left(-i\frac{\Delta t}{2}\sigma_z\right) = \sigma_0 \cos\left(\frac{\Delta t}{2}\right) - i\sigma_z \sin\left(\frac{\Delta t}{2}\right), \quad (59)$$

where σ_0 is the 2x2 unit matrix. Furthermore, the evolution operator $U_I(t) = U_0^{-1}(t)U(t)$ is generated by the Hamiltonian

$$H_I(t) = U_0(t)^{-1}V(t)U_0(t) = v_g(t)\sigma^+ + v_g^*(t)\sigma^-, \quad (60)$$

with

$$v_g(t) = \frac{g}{2}\tilde{f}(t)e^{i\Delta t}, \quad (61)$$

which is the entry in the first column of Table I. Since $|g| < 1$, the convergence condition Eq. (15) is satisfied for the whole interval $t \in [0, 2\pi]$:

$$\int_0^t |v_g(s)|ds \leq \int_0^t \frac{|g|}{2}ds = \frac{|g|t}{2} < \pi. \quad (62)$$

This inequality holds without any condition for the magnitude of Δ .

In order to find the angle-axis parameterization in Eq. (3), one needs to solve the BCH problem⁷², i.e., to use

$$\exp(-i\theta\vec{n} \cdot \vec{\sigma}) = \exp(-i\theta_0\vec{n}_0 \cdot \vec{\sigma}) \exp(-i\theta_I\vec{n}_I \cdot \vec{\sigma}) \quad (63)$$

and to determine θ and \vec{n} from the pairs (θ_0, \vec{n}_0) and (θ_I, \vec{n}_I) . Using the properties of the Pauli matrices, we get

$$\cos \theta = \cos \theta_0 \cos \theta_I - \sin \theta_0 \sin \theta_I \vec{n}_0 \cdot \vec{n}_I, \quad (64)$$

$$\begin{aligned} \sin \theta \vec{n} &= \sin \theta_0 \cos \theta_I \vec{n}_0 + \cos \theta_0 \sin \theta_I \vec{n}_I \\ &+ \sin \theta_0 \sin \theta_I \vec{n}_0 \times \vec{n}_I. \end{aligned} \quad (65)$$

θ_0 and \vec{n}_0 will be read off from the unitary transformation matrix U_0 . For example, from Eq. (59) one finds

$$\theta_0(t) = \frac{\Delta t}{2}, \quad \vec{n}_0 = \hat{e}_z. \quad (66)$$

θ_I and \vec{n}_I , on the other hand, will be determined from the ME, i.e., from the insertion of Eq. (9) into Eqs. (7,8). The application of Eqs. (64,65) will be illustrated below in the discussion of the Rabi model.

Region II: $|\Delta| < \omega$

Next we consider the regime $|\Delta| < 1$. To reuse the above derivation, we exchange σ_x and σ_z in Eq. (1) by the 2x2 Hadamard matrix $H_2 \equiv \frac{1}{\sqrt{2}}(\sigma_x + \sigma_z)$, via

$$H_2 \sigma_x H_2 = \sigma_z, \quad H_2 \sigma_z H_2 = \sigma_x. \quad (67)$$

This is a time-independent similarity transform and does not affect any physical observables, as well as the quasienergy. Compared to the previous regime $|g| < 1$, we switch also H_0 and V , namely we set

$$H_0(t) = \frac{g\tilde{f}(t)}{2}\sigma_z, \quad V = \frac{\Delta}{2}\sigma_x, \quad (68)$$

and stress that the unperturbed Hamiltonian is now time-dependent, although it does not contain non-commuting operators. Thus a transformation into the interaction picture using

$$\begin{aligned} U_0(t) &= \exp\left(-i\frac{g\tilde{F}(t)}{2}\sigma_z\right) \\ &= \sigma_0 \cos\left(\frac{g\tilde{F}(t)}{2}\right) - i\sigma_z \sin\left(\frac{g\tilde{F}(t)}{2}\right), \end{aligned} \quad (69)$$

with

$$\tilde{F}(t) \equiv \int_0^t \tilde{f}(s) ds \quad (70)$$

yields

$$H_I(t) = v_\Delta(t)\sigma^+ + v_\Delta^*(t)\sigma^-, \quad (71)$$

where

$$v_\Delta(t) = \frac{\Delta}{2} e^{ig\tilde{F}(t)}. \quad (72)$$

Again, $|\Delta| < 1$ ensures that the ME for $U_I(t)$ converges within a period.

Region III: $\omega < |g|$ **and** $\omega < |\Delta|$

The last parameter regime that we consider is given by $\omega < |g|$ and $\omega < |\Delta|$, which means the driving is relatively slow-varying. We expect the adiabatic picture explained in Sec. III to be a suitable choice. We repeat Eq. (22), but now for the time-evolution over one period:

$$U(T) = \Psi(T)\Phi(T)U_a(T)\Psi^\dagger(0).$$

Since the Hamiltonian is periodic, we have $\Psi(T) = \Psi(0)$. Furthermore, $\Phi(T)$ contributes the dynamical phase, whereas under the adiabatic approximation $U_a(T)$ is only responsible for the geometrical, so-called Berry phase⁶⁵. Thus, in the adiabatic limit, we have

$$\epsilon = \frac{1}{T}[\varphi(T) + \varphi_{\text{Berry}}(T)] \quad (73)$$

for the quasienergy. For more detailed discussion of the dynamical/geometrical decomposition of the Floquet quasienergy, we refer the reader to⁷³. In the following, we apply the ME to the Rabi model and at the end of the next subsection, we show how to go beyond the adiabatic approximation.

B. Semiclassical Rabi Model

In the semiclassical Rabi model, the shape function $\tilde{f}(t)$ can be chosen either as $\cos\omega t$ or $\sin\omega t$. The concrete choice does not affect the *exact* analytic/numeric value of the quasienergy and we will be using

$$\tilde{f}(t) = \cos\omega t \quad (74)$$

in the following. Yet we would like to point out that employing $\tilde{f}(t) = \sin\omega t$, instead, may lead to qualitative differences for the ME, since sine and cosine functions possess different symmetries in the interval $[0, \pi]$, see also Appendix B.

For either choice, the Hamiltonian Eq. (1) obeys the so-called generalized parity (GP) symmetry

$$PH(t + \pi)P = H(t), \quad (75)$$

where $P = \sigma_z$. The relevance of this symmetry in the context of periodically driven tunneling was highlighted in⁷⁴. Based on a classic argument by von Neumann and Wigner⁷⁵,

it was shown that GP symmetry allows for exact crossings of quasienergies along one-dimensional manifolds in a two-dimensional parameter space made up of frequency and driving strength⁷⁶. In the two-level system studied herein similar crossings may occur^{22,77}. The two parameters to be varied herein are driving strength g and Δ , i.e., the unperturbed level splitting, however. By using the GP symmetry one can prove that ϵ is an odd function of Δ and an even function of g , namely,

$$\epsilon(\Delta, g) = \epsilon(\Delta, -g) = -\epsilon(-\Delta, g). \quad (76)$$

Thus we may focus on the case where all parameters are positive valued. However, as will be seen below, the existence of the GP symmetry also leads to some subtleties that require special attention.

Exact analytic results

As a reference to compare our ME results to, we reproduce the exact solution for the quasienergy, given by Schmidt and collaborators^{78,79}. It was found that

$$\epsilon(\Delta, g) = \frac{1}{\pi} \sin^{-1} \left[\sqrt{2} \Delta \operatorname{Re} \left(e^{ig} \eta_+(g, \Delta) \eta_-(g, \Delta) \right) \right] \quad (77)$$

holds for the quasienergy, where

$$\begin{aligned} \eta_{\pm}(\Delta, g) &:= \operatorname{HeunC}(\pm\mu_0, \mu_1, b_0, b_1, a; z = \frac{1}{2}), \\ \mu_0 = \mu_1 &= \frac{1}{2}, \quad a = 2ig, \\ b_0 &= -\frac{1}{8}(4ig + 2\Delta^2 + 1), \quad b_1 = ig. \end{aligned}$$

Here "HeunC" denotes Heun's confluent function⁸⁰, which is implemented in standard mathematical software packages and/or can be programmed via Taylor expansion. In Fig. 3 the exact analytical quasienergy $\epsilon(\Delta, g = 1)$ is depicted as a function of Δ . As shown by the magnifying view in panel (b) of the figure, near the boundary of the first Brillouin zone (extending from -0.5 to 0.5) crossings are avoided, as to be expected from the argument given in Appendix C.

We note in passing that the exact quasienergies can also be calculated numerically by diagonalizing the so-called Floquet matrix⁴⁰. Especially for large values of g , the number of 2x2 sub-matrices to be taken into account to achieve convergence increases considerably, however.

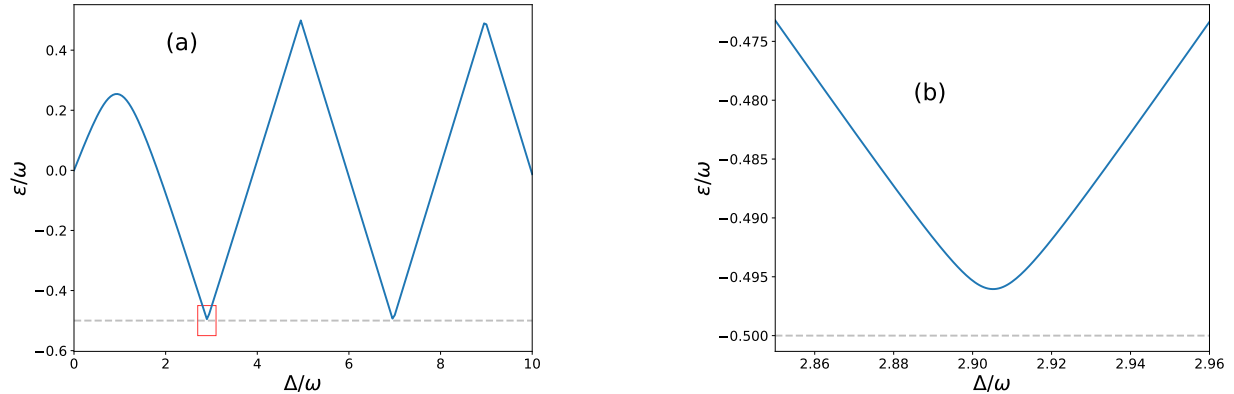


FIG. 3: Exact results for the quasienergy of the Rabi model at $g/\omega = 1$ as a function of Δ . Panel (b) shows a magnified view for the boxed region in panel (a), displaying an avoided crossing.

Region I

Applying the ME, firstly, we consider the weak driving case I, i.e., $|g| < \omega$. We recall that $U_0(t)$ is then given by Eq. (59) while $U_I(t)$ has to be determined via the ME. Once we obtain the MC $A_I(2\pi)$ and $C_I(2\pi)$ as well as $\theta_I(2\pi)$ from the ME for $U_I(2\pi)$, from Eq. (64), the quasienergy follows to be

$$\epsilon_{2\pi} = \frac{1}{2\pi} \cos^{-1} \left[\cos(\pi\Delta) \cos \theta_I - C_I \sin(\pi\Delta) \frac{\sin \theta_I}{\theta_I} \right], \quad (78)$$

and is thus given in terms of easily accessible trigonometric and inverse trigonometric functions and the sinc function. We explicitly denote the fact that the quasienergy is extracted from the time-evolution operator over the full period by the index 2π . Fig. 4 (a) shows the results for the first three orders of the Magnus approximation for $g = 1$ at the border of the first domain and up to $\Delta/\omega \approx 3$, i.e., up to the avoided crossing highlighted in Fig. 3 (b). For smaller $|\Delta|$ the ME converges faster and the results are more accurate. As the order increases, the accuracy does improve. In particular, the second order is needed to observe the shift of the position of the avoided crossing, which corresponds to the Bloch-Siegert shift⁹, originally introduced in nuclear magnetic resonance and discussed in the present context by Shirley⁷⁰.

There is an apparent flaw in the results presented in panel (a) of Fig. 4, however. This is

the fact that the *exact* crossings at $\Delta/\omega \approx 1.82$ are artificially *avoided* by the Magnus results. We note in passing that a similar issue occurs for another related model⁴³. This flaw arises because the GP symmetry involves a time-translation operation. Unlike PT symmetry, it is artificially violated under finite order Magnus approximation due to truncation errors. To fix the issue, we have to explicitly maintain the GP symmetry. In order to do so, we consider the time-evolution operator U_0 over half a period and from Eq. (59) we read off

$$\theta_0 = \frac{\Delta\pi}{2}, \quad \vec{n}_0 = \hat{e}_z. \quad (79)$$

In addition, we have to determine θ_I and \vec{n}_I for $U_I(\pi)$ via the ME according to Eqs. (7,8). Then applying $\hat{e}_z \cdot$ to both sides of Eq. (65) we have

$$\hat{e}_z \cdot (\sin \theta \vec{n}) = \cos \theta_I \sin \theta_0 + \cos \theta_0 \sin \theta_I \hat{e}_z \cdot \vec{n}_I. \quad (80)$$

Furthermore, in Appendix C we prove that, in the presence of GP symmetry,

$$\text{tr}[PU(\pi)] = \sin(\epsilon\pi) = \vec{n}_P \cdot (\sin \theta \vec{n}) \quad (81)$$

holds and we can thus extract the quasienergy from the time-evolution operator over half a period, as has been noted also in⁷⁹. Here $\vec{n}_P = \hat{e}_z$ is determined by $P = \vec{n}_P \cdot \vec{\sigma}$. Finally, comparing Eq. (80) with Eq. (81), we get

$$\epsilon_\pi = \frac{1}{\pi} \sin^{-1} \left[\sin \left(\frac{\pi\Delta}{2} \right) \cos \theta_I + C_I \cos \left(\frac{\pi\Delta}{2} \right) \frac{\sin \theta_I}{\theta_I} \right], \quad (82)$$

where the MC are now all taken at time $t = T/2 = \pi$. The complexity of the result is similar to the one of Eq. (78) and the results gained from the improved formula are depicted in panel (b) of Fig. 4. As expected, now the exact crossings are properly reproduced and in addition also the overall accuracy has improved due to the extra work. The second order results, e.g., are so well-converged that they barely can be distinguished from the exact ones in panel (b) over the whole range of Δ . Going to third order the results are graphically almost indistinguishable from the exact ones.

Region II

Secondly, we compute the quasienergy for the parameter regime of region II, i.e., $|\Delta| < \omega$ with the corresponding identification of $v(t) = v_\Delta(t)$ given in the second column of Table I.

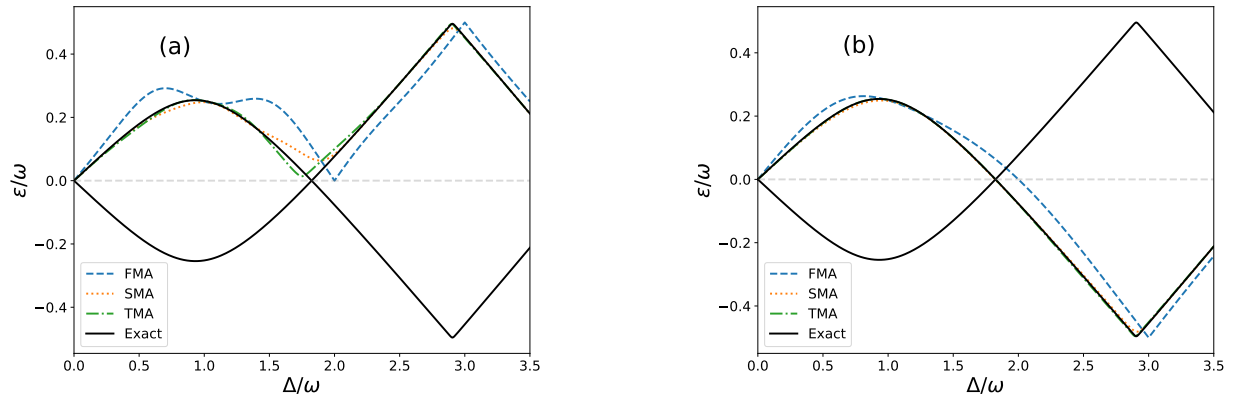


FIG. 4: Quasienergies for $g = 1$: (a) exact result for ϵ and $-\epsilon$ (solid black lines) and Magnus approximations of different order based on the picture appropriate for region I (1st order: dashed blue, 2nd order: dotted orange, 3rd order: dash-dotted green) for ϵ , directly computed from $U(2\pi)$; (b) same as (a) but with Magnus approximations with generalized parity symmetry explicitly maintained by using $U(\pi)$ for the determination of ϵ (see text).

Specifically, with $\tilde{f}(t) = \cos(t)$ yielding $\tilde{F}(t) = \sin(t)$, we get

$$v_{\Delta}(t) = \frac{\Delta}{2} e^{i \sin t}. \quad (83)$$

Furthermore, according to Eq. (69),

$$\theta_0(t) = \frac{g}{2} \tilde{F}(t), \quad \vec{n}_0 = \hat{e}_z, \quad (84)$$

follows, in contrast to Eq. (66).

For the discussion of the FMA in the present case we start with the time-evolution operator over the full period. We note that here $\theta_0(2\pi) = 0$ and hence $H_I(t)$ remains periodic, which is a direct result by the GP symmetry. Thus from Eq. (56), we can directly read off

$$\epsilon_{2\pi} = \frac{1}{2\pi} \theta_I(2\pi). \quad (85)$$

Using Eqs. (7) and (12), the first order Magnus approximation thus generally yields

$$\epsilon_{2\pi}^{\text{FMA}} = \frac{|A_I^{\text{FMA}}(2\pi)|}{2\pi} = \frac{\Delta}{4\pi} \left| \int_0^{2\pi} \exp[ig\tilde{F}(\tau)] d\tau \right|, \quad (86)$$

which under cosine-driving becomes

$$\epsilon_{2\pi}^{\text{FMA}} = \frac{\Delta}{2} \frac{1}{\pi} \left| \int_0^{\pi} \cos(g \sin \tau) d\tau \right| = \frac{\Delta}{2} J_0(g). \quad (87)$$

This is the zeroth-order Bessel function⁸¹ expression for the quasienergy of the semiclassical Rabi model, a result which has been found using perturbation theory more than sixty years ago by Shirley⁷⁰ and can also be extracted from the Heun function solution in the limit $\Delta \rightarrow 0$ ⁷⁹. A physical interpretation of Eq. (86) has been given in terms of an effective tunneling rate that vanishes at the zeros of J_0 ^{21,22,26,82}.

With the ME it is straightforward to find next order correction terms, yet we refrain from going to higher order for $U_I(2\pi)$ here and turn to the approach with the GP symmetry explicitly maintained. To make progress, we note that we have exchanged σ_x and σ_z by Eq. (67) for region II and thus the representation of the parity operator changes accordingly, i.e.,

$$P = \sigma_x, \quad \vec{n}_P = \hat{e}_x. \quad (88)$$

In the present case we have $\theta_0(\pi) = 0$ and thus Eq. (65) simplifies considerably and the corresponding quasienergy reads

$$\epsilon_\pi = \frac{1}{\pi} \sin^{-1} \left[\text{Re}(A_I) \frac{\sin \theta_I}{\theta_I} \right]. \quad (89)$$

Herein, the MC are again taken at $t = \pi$ as indicated by the quasienergy index. To compare Eq. (86) with Eq. (89), for the latter the first order ME contribution reads

$$\begin{aligned} A_I^{\text{FMA}}(\pi) &= \frac{\Delta}{2} \int_0^\pi \exp[ig \sin t] dt \\ &= \frac{\Delta\pi}{2} [J_0(g) + iH_0(g)], \end{aligned} \quad (90)$$

where H_0 is the zeroth-order Struve function⁸¹. As depicted in Fig. 5, the first-order symmetry conserving result is slightly more accurate than the one based only on J_0 , at the cost of a more complicated form for ϵ .

Furthermore, since $\cos(\pi/2 + t) = -\cos(\pi/2 - t)$, $H(t)$ and $H_I(t)$ possess PT symmetry with respect to the reflection time $t = \pi/2$ in the interval $t \in [0, \pi]$. Therefore, as explained in Appendix B, the $C_n(\pi)$ coefficients automatically vanish. That is, even-order ME terms for $U(\pi)$ are all zero and thus the SMA does not improve on FMA. We stress, however, if $\tilde{f} = \sin \omega t$ instead of $\tilde{f} = \cos \omega t$ is adopted, the symmetry is realized in another way.

In Fig. 5 for $\Delta = \omega$, i.e., at the border of region II, we observe that especially for small values of g there is still a discrepancy between the exact result and the lower order Magnus approximations. In contrast, TMA leads to a dramatic reduction in error, including the

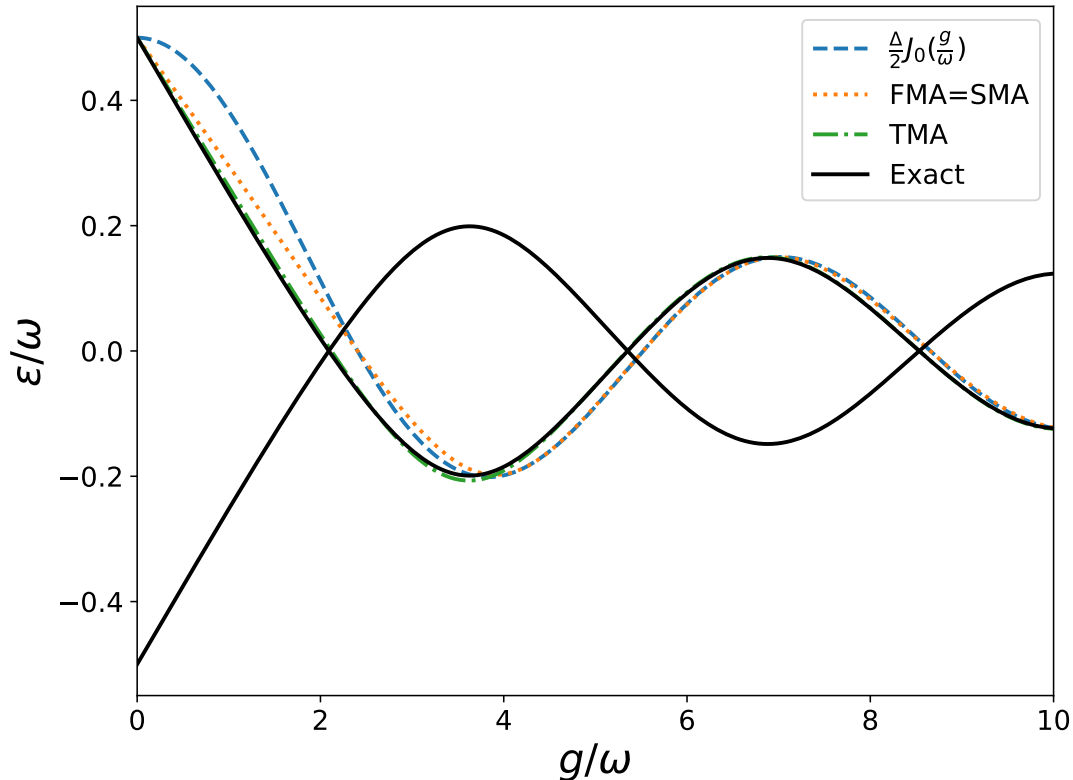


FIG. 5: Quasienergy of the semiclassical Rabi model at $\Delta = \omega$ as a function of g : exact result for ϵ and $-\epsilon$ (solid black lines) and Magnus approximations of different order based on the picture appropriate for region II: 1st order extracted from time evolution over 2π : dashed blue, 1st (equal to 2nd) order with the generalized parity symmetry explicitly maintained: dotted orange, 3rd order with the generalized parity symmetry explicitly maintained: dash-dotted green.

correction of the shifted relative extrema as well as the inaccurate positions of the first three exact quasi energy crossings observed in FMA. It is also noteworthy that all orders of the symmetry conserving calculation show a nonzero slope at $g = 0$, in agreement with the exact result, whereas this feature is absent when the ME is directly applied to $U(2\pi)$. We note that for smaller values of $\Delta \ll 1$ inside region II, FMA is a very good approximation already (not shown).

The non-zero slope at $g = 0$ is related to a coincidental crossing on the boundary of 1st BZ, i.e. $\epsilon = 0.5\omega$. Actually, when $g = 0$ the quasienergy obviously coincides with the static

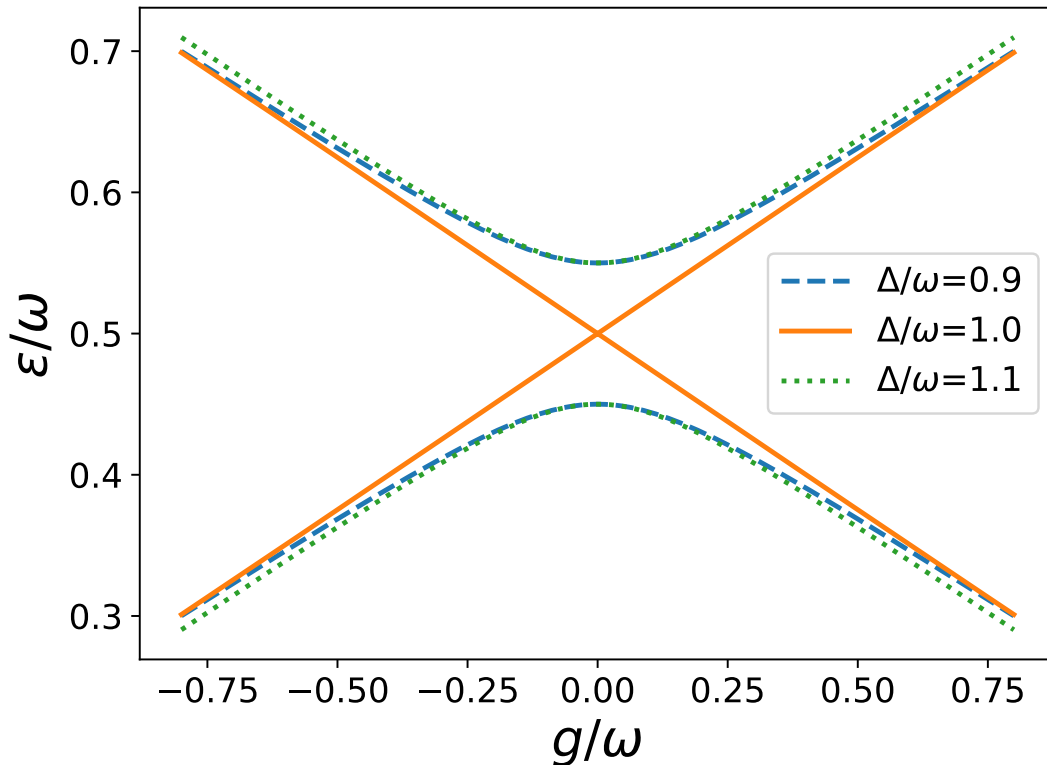


FIG. 6: Exact results for ϵ in the Rabi model as a function of g for different fixed Δ : when $\Delta = \omega$ a coincident crossing takes place at $g = 0$, which results in non-zero slope (solid yellow line); for most values of Δ , the crossing is avoided and the slope is zero ($\Delta = 0.9\omega$: dashed blue, $\Delta = 1.1\omega$: dotted green).

energy, namely,

$$\epsilon_{g=0} = \pm \frac{\Delta}{2} \pmod{\omega}. \quad (91)$$

For fixed Δ , two values (modulo ω) of ϵ must vary smoothly with g by virtue of the smooth dependence of solutions on parameters in linear systems. On the other hand, according to Eq. (76), in general ϵ is an even function of g and thus has vanishing derivative at $g = 0$. The only exception arises when crossings take place, i.e., when Δ/ω is an integer. This is further illustrated in Fig. 6 by the exact results of ϵ . Furthermore, we remark that the crossing at $\epsilon = 0.5\omega$ restricts the convergence radius of the ME⁵⁵. When convergence of the ME is not guaranteed, spurious crossings may appear in the quasienergy spectrum, resulting in a complete loss of accuracy, as depicted in Fig. 7, where the different orders of the ME for $\epsilon_{2\pi}$ using the picture appropriate for region II are compared in the case $\Delta = 1.2\omega$ (which

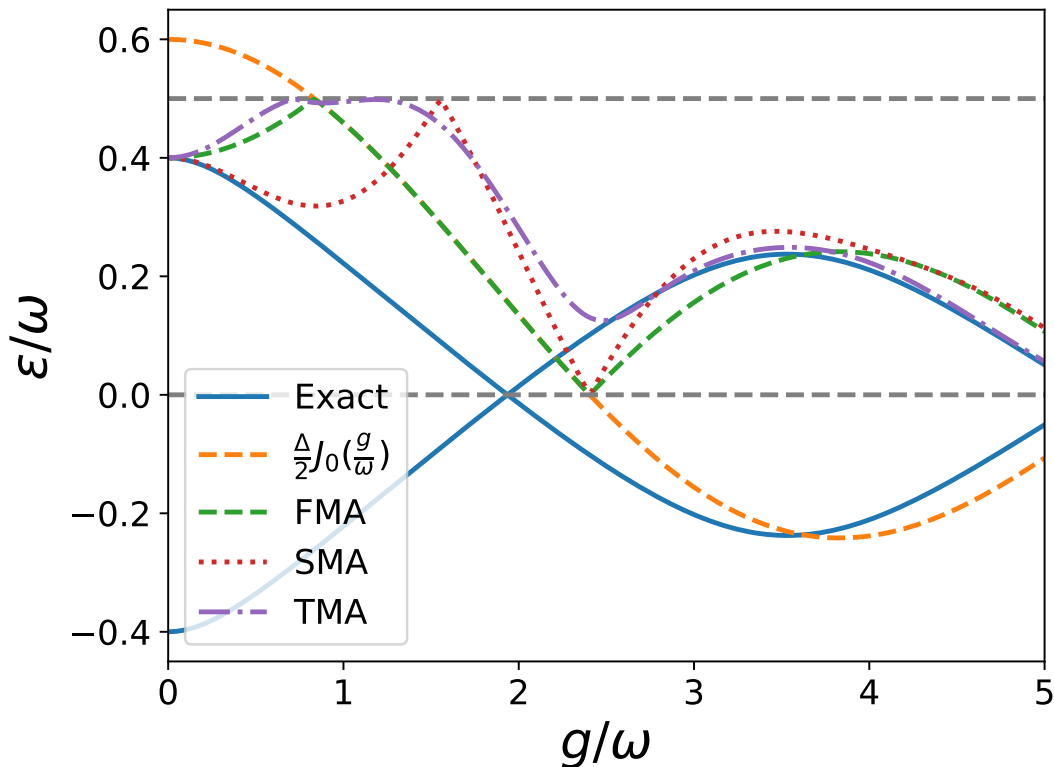


FIG. 7: Different results for $\epsilon_{2\pi}$ in the Rabi model based on the picture appropriate for region II as a function of g for $\Delta/\omega = 1.2$, outside of region II. Exact result for ϵ and $-\epsilon$ (solid blue lines) and Magnus approximations of different order (Bessel function results: dashed orange, 1st order: dashed green, 2nd order: dotted red, 3rd order: dash-dotted purple) for ϵ , directly computed from $U(2\pi)$

is outside of region III!).

Region III

Finally we address the adiabatic picture, which is expected to be a good approximation in region III, when $|g| > \omega$, $|\Delta| > \omega$. For this regime we choose the shape function as $\tilde{f}(t) = \cos(t)$ which is monotonic for $t \in [0, \pi]$ so that that ME can be safely applied. As explained in Sec. III, on the LZSM problem, the ME for $U_a(\pi)$ actually converges for the entire (g, Δ) plane.

Firstly, in this case, the dynamical phase from Eq. (20) reads

$$\begin{aligned}\varphi(t) &= \frac{1}{2} \int_0^t \sqrt{\Delta^2 + g^2 \cos^2 r} dr \\ &= \frac{1}{2} \int_0^t \sqrt{\Delta^2 + g^2 - g^2 \sin^2 r} dr = \frac{m}{2} E(t, k),\end{aligned}\quad (92)$$

with $m := \sqrt{\Delta^2 + g^2}$, $k := g^2/m^2$ and where E is Jacobi's *incomplete* elliptic integral of the second kind⁸¹. Secondly, we recall the transform into the adiabatic picture from Eq. (22), now taken at the half period:

$$U(\pi) = \Psi(\pi)\Phi(\pi)U_a(\pi)\Psi^\dagger(0).\quad (93)$$

With the GP symmetry, one may verify that

$$P\Psi(\pi)P = \Psi(0)$$

and therefore

$$PU(\pi) = \Psi(0)\Phi(\pi)U_a(\pi)\Psi^\dagger(0) = \Phi(\pi)U_a(\pi).$$

Here we omit the similarity transform, which does not change the trace in Eq. (81). Using Eq. (65) and Eq. (81), we can again extract the quasienergy from the time-evolution operator over half a period according to

$$\epsilon_\pi = \frac{1}{\pi} \sin^{-1} \left\{ \sin[\varphi(\pi)] \cos \theta_a + C_a \cos[\varphi(\pi)] \frac{\sin \theta_a}{\theta_a} \right\}.\quad (94)$$

The plain adiabatic approximation corresponds to the zeroth order Magnus approximation (ZMA) ($A_a = C_a = \theta_a = 0$) and in this limit, from Eq. (94), we get

$$\epsilon_\pi^{\text{ZMA}} = \frac{1}{\pi} \varphi(\pi) \pmod{1},\quad (95)$$

which by using Eq. (92), is given in terms of the *complete* elliptic integral of the second kind. The quasienergy thus is proportional to the dynamical phase only, as can be seen by comparison with Eq. (73) and the above ZMA result is analogous to the one given by Shirley in his Eqn. (28)⁷⁰, which was also derived for small frequencies.

Fig. 8 shows the increasing accuracy of the zeroth order result for large Δ , i.e., in the adiabatic limit of relatively small ω . Higher order Magnus approximations, on the other hand, also properly reveal the avoided crossings (between quasienergies from different BZs) at the extrema, with the most prominent ones at small values of Δ . It turns out that even for very small $\Delta/\omega \ll 1$, the SMA is almost exact in the present case, thus vastly extending the applicability of the adiabatic approximation.

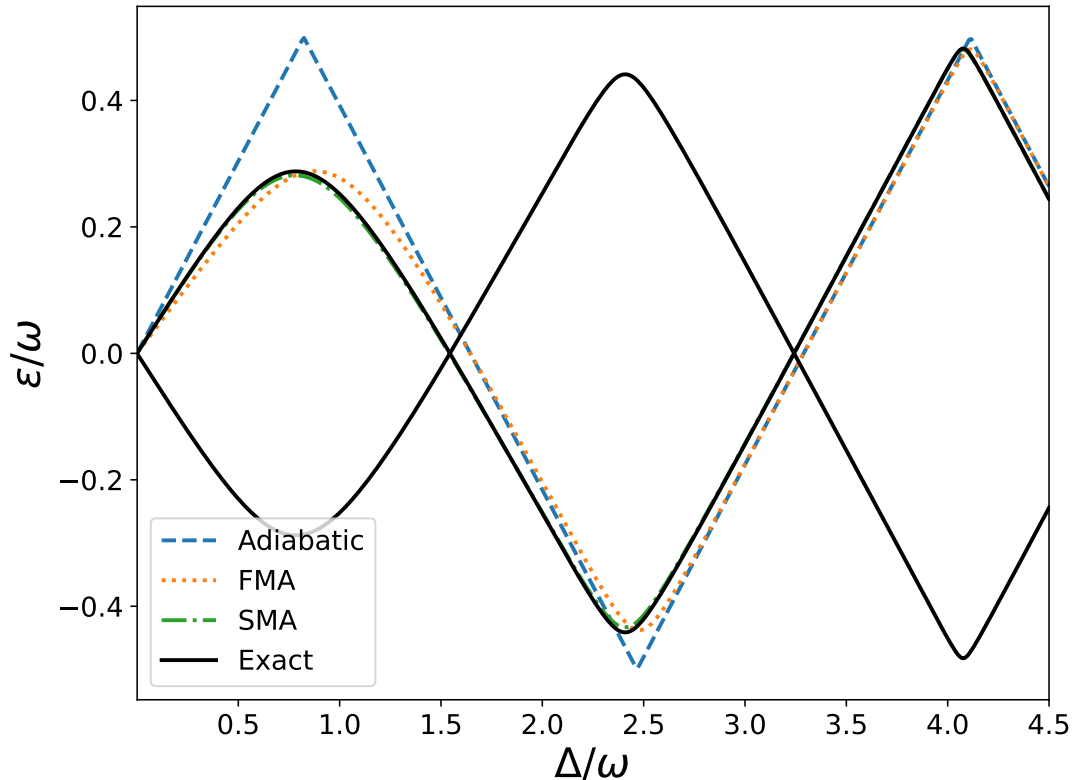


FIG. 8: Quasienergies of the Rabi model as a function of Δ along the diagonal in the parameter plane displayed in Fig. 2, i.e., for $g = \Delta$: exact result for ϵ and $-\epsilon$ (solid black lines) and Magnus approximations of different order (0th order (ZMA): dashed blue, 1st order: dotted orange, 2nd order: dash-dotted green) in the adiabatic picture

V. CONCLUSIONS AND OUTLOOK

In this study we have demonstrated that the Magnus expansion may serve as a highly accurate approximation for the (semi-)analytical determination of non-perturbative transitions as well as of the quasienergy spectrum in (single-axis) driven two-level systems already for relatively low orders if symmetry properties are taken care of. For both models that we studied, the third order Magnus approximation was sufficient for almost complete agreement with the known exact analytical results in all of parameter space.

For the Landau-Zener problem, we have, e.g., shown that higher order Magnus approximations can not only accurately reproduce transition probabilities, but (from second order on) also yield the Stokes phase quite accurately. The PT symmetry of the model is preserved

by the ME to all orders and the convergence criterion is always met. This is true for every monotonic drive and if this condition is not fulfilled, the drive can be split into monotony intervals and the Magnus approximations can be used for the separate domains.

It is well-known that the lowest order Magnus approximation for the semiclassical Rabi model has a similar accuracy as the rotating wave approximation^{71,83}. By studying the time-evolution operator over one period up to higher order Magnus approximation, we have investigated the entire parameter regime of this model and have shown that exact and avoided crossings can be reproduced to a high degree. Especially, the Bloch-Siegert shift is quite accurately reproduced using a next-to-leading order Magnus approximation. The correct qualitative as well as quantitative prediction of exact crossings calls for a ME based on the time-evolution operator over only half the period, however, which allows to restore the generalized parity symmetry that is lost otherwise. Results of third order are almost indistinguishable from the exact analytic results based on the confluent Heun function for the whole parameter space. The quality of the results for the quasienergies is thus similar as that of previous iterative approaches⁸⁴ but there is no restriction to the applicability of the ME if appropriate picture transformations are performed. If a picture is applied in a domain where it is not appropriate, the results are deteriorating rapidly as exemplified in the case of the Rabi model. An especially appealing picture is the adiabatic one, as has already been noted by Klarsfeld and Oteo, who found that the ME in the adiabatic pictures dramatically improves on perturbation theory for a spin 1/2 system in a rotating magnetic field⁶³. We have shown herein that, in the Rabi case and in the adiabatic picture, the second order ME result already gives almost perfect agreement with the exact analytic quasienergies in the whole parameter range.

On a technical note, we have emphasized the importance of the convergence condition, picture transformations and the maintenance of symmetry of the underlying problem. For monotonic driving, it has been shown that convergence criteria can be easily satisfied. However, in quantum control, the driving field is often modeled as a carrier oscillation modulated by a slowly varying envelope. It remains an important problem whether one can gain qualitative insights into the system's behavior from the driving fields. A fully satisfactory answer remains elusive; nevertheless, our method appears promising and warrants further investigation. A very interesting question, e.g., is if the application of the ideas herein improves on the findings by Begzjav and Eleuch on the two-level dynamics under an off-resonant pulse

in the presence of a dissipative channel⁴⁸.

A simple yet effective twist of this study is to employ the $\mathfrak{su}(2)$ algebra to decompose the Magnus expansion. This procedure can be generalized to the non-Hermitian case⁸⁵, without significant changes. Furthermore, also multiple axis driving can and should be studied along the lines that we used herein. In addition, it seems to be a natural extension to apply the $\mathfrak{su}(3)$ algebra⁸⁶ to treat three-level systems. Furthermore, the Magnus coefficients are very often expressed as multi-variate oscillating integrals. This indicates that that the Magnus approximation often becomes accurate under both large and small parameter limits, as we have noticed in the results of the LZSM and Rabi model. An error estimation analysis^{54,87} seems very appealing, yet it is far beyond the present study's scope.

Finally, in⁸⁸ the ME is used to design an effective driving along a third axis from a commutator of Pauli σ_x and σ_z matrices. To show this, the authors employed the Magnus-Floquet expansion to second order, whose accuracy depends on frequency. Yet our study shows that the validity of the ME is in general not limited by the range of frequency, which might trigger new insights for the design of effective counter-diabatic Hamiltonians⁸⁹.

Appendix A: $\mathfrak{su}(2)$ decomposition of the Magnus expansion

Owing to the Schrödinger equation for the time-evolution operator $U(t)$ with initial condition $U(t_0) = I$, the Magnus operator $\Omega(t)$ in Eq. (2) must fulfill¹

$$-i\dot{\Omega}(t) = \sum_{j=0}^{\infty} (-i)^j \frac{B_j}{j!} \text{ad}_{\Omega}^j(H(t)), \quad \Omega(t_0) = 0, \quad (\text{A1})$$

where the adjoint operator is defined by $\text{ad}_{\Omega}(\cdot) = [\Omega, \cdot]$, $\text{ad}_{\Omega}^k(\cdot) = [\Omega, \text{ad}_{\Omega}^{k-1}(\cdot)]$ and $B_0 = 1, B_1 = -1/2, B_2 = 1/6, B_3 = 0, B_4 = -1/30, \dots$ are Bernoulli numbers.

Replacing the Hamiltonian $H(t)$ by $\lambda H(t)$ (and taking λ equal to 1 in the end), the Magnus expansion amounts to finding a power series expansion for the solution of Eq. (A1),

$$\Omega(t) = \sum_{n=1}^{\infty} \lambda^n \Omega_n(t). \quad (\text{A2})$$

To each order, $\Omega_n(t)$ can be iteratively determined as integrals of Lie brackets¹ by the Hamiltonian at different times. In order to find Ω_n , one needs to collect all the λ^n contributions from ad_{Ω}^j in Eq. (A1). Following the notation of Klarsfeld and Oteo⁹⁰, we get

$$\dot{\Omega}_1(t) = H(t), \dot{\Omega}_n(t) = \sum_{j=1}^{n-1} \frac{B_j}{j!} S_n^{(j)}(t) \quad (n \geq 2), \quad (\text{A3})$$

where the quantities

$$S_n^{(j)}(t) := \sum_{m=1}^{n-j} (-i) [\Omega_m(t), S_{n-m}^{(j-1)}(t)], \quad 1 \leq j \leq n-1 \quad (\text{A4})$$

are to be determined recursively with initial conditions $S_1^{(0)}(t) \equiv H(t)$, $S_n^{(0)}(t) := 0$ ($n \geq 2$).

For reference, the first three orders read⁶⁰

$$\Omega_1(t) = \int_{t_0}^t dt_1 H(t_1), \quad (\text{A5})$$

$$\Omega_2(t) = -\frac{i}{2} \int_{t_0}^t dt_1 \int_{t_0}^{t_1} dt_2 [H(t_1), H(t_2)], \quad (\text{A6})$$

$$\begin{aligned} \Omega_3(t) = & -\frac{1}{6} \int_{t_0}^t dt_1 \int_{t_0}^{t_1} dt_2 \int_{t_0}^{t_2} dt_3 \\ & \left([H(t_1), [H(t_2), H(t_3)]] \right. \\ & \left. + [H(t_3), [H(t_2), H(t_1)]] \right). \end{aligned} \quad (\text{A7})$$

Now we specialize the recursion relation to a traceless Hermitian Hamiltonian. From Eq. (A4) it follows that $S_n^{(j)}$ is also traceless and Hermitian, and thus it can be decomposed as

$$S_n^{(j)} = a_n^{(j)}(t)\sigma_+ + a_n^{(j)*}(t)\sigma_- + c_n^{(j)}(t)\sigma_z. \quad (\text{A8})$$

Then the decomposition of $\Omega_n(t)$ follows to be

$$\Omega_n(t) = A_n(t)\sigma_+ + A_n^*(t)\sigma_- + C_n(t)\sigma_z, \quad (\text{A9})$$

where

$$A_n(t) = \sum_{j=0}^{n-1} \frac{B_j}{j!} \int_{t_0}^t a_n^{(j)}(\tau) d\tau, \quad (\text{A10})$$

$$C_n(t) = \sum_{j=0}^{n-1} \frac{B_j}{j!} \int_{t_0}^t c_n^{(j)}(\tau) d\tau. \quad (\text{A11})$$

With these definitions and using the $\mathfrak{su}(2)$ algebra in Eq. (5), the recursion relation in Eq. (A4) can be reduced into commutator-free form according to

$$a_n^{(j)}(t) = 2i \sum_{m=1}^{n-j} \left[C_m(t) a_{n-m}^{(j-1)}(t) - A_m(t) c_{n-m}^{(j-1)}(t) \right], \quad (\text{A12})$$

$$c_n^{(j)}(t) = 2 \sum_{m=1}^{n-j} \text{Im} \left[A_m(t) a_{n-m}^{(j-1)*}(t) \right], \quad (\text{A13})$$

$$a_n^{(0)}(t) = c_n^{(0)}(t) = 0 \quad (2 \leq n, 1 \leq j \leq n-1). \quad (\text{A14})$$

Higher order Magnus expansions for two-level quantum dynamics

Recalling that $S_1^{(0)}(t) \equiv H(t)$, the initial conditions for the recursion are determined by the $\mathfrak{su}(2)$ decomposition

$$H(t) = a_1^{(0)}(t)\sigma^+ + a_1^{(0)*}(t)\sigma^- + c_1^{(0)}(t)\sigma_z \quad (\text{A15})$$

of the Hamiltonian.

Appendix B: Symmetry of the Magnus operator

For the reader's convenience, we repeat the definition of PT symmetry

$$PH^*(-t)P = H(t), \quad (\text{B1})$$

from Eq. (45), where the parity operator is Hermitian as well as unitary, i.e., it satisfies

$$P^\dagger = P, \quad P^2 = \mathbb{I}. \quad (\text{B2})$$

In addition in this appendix we assume that P has a real (matrix) representation, i.e.,

$$P^* = P \quad (\text{B3})$$

is assumed to hold. Based on Eq. (B1) one may directly verify the following symmetry on the time-evolution operator level:

$$U^*(-t, 0) = PU(t, 0)P. \quad (\text{B4})$$

One may justifiably ask how this symmetry is carried over to the Magnus operator level.

To answer this question, we consider the Magnus operator on a symmetric time interval $[-t_f, t_f]$. For simplicity, we denote

$$S \equiv U(t_f, -t_f) \equiv \exp(-i\Omega). \quad (\text{B5})$$

By the group property of the evolution operator, we have

$$\begin{aligned} S &= U(t_f, 0)U(0, -t_f) \\ &= U(t_f, 0)U^{-1}(-t_f, 0) \\ &= U(t_f, 0)P[U^*(t_f, 0)]^{-1}P. \end{aligned} \quad (\text{B6})$$

In the last step we have used Eq. (B4) and the properties of P . It thus follows that

$$[S^*]^{-1} = PSP. \quad (\text{B7})$$

On the other hand, by the definition of matrix exponent we have

$$[S^*]^{-1} = \exp(-i\Omega^*) \quad (\text{B8})$$

and from (B5)

$$PSP = \exp[-i(P\Omega P)]. \quad (\text{B9})$$

Comparing the two last equations, finally, we conclude that

$$\Omega^* = P\Omega P. \quad (\text{B10})$$

Note that Ω as well as Ω^* are both associated with the time interval $[-t_f, t_f]$. From the power series expansion of Ω , given in Eq. (A2), it follows that the property Eq. (B10) holds to each order. We note in passing that to reach the final conclusion, the Hamiltonian does not have to be Hermitian.

To illustrate the application of Eq. (B10), we elaborate on the PT symmetry of the two-level Hermitian systems from the main text. For this, we rewrite Eq. (6) as

$$\Omega = \text{Re}(A)\sigma_x - \text{Im}(A)\sigma_y + C\sigma_z, \quad (\text{B11})$$

and thus (note that C is real-valued) we find

$$\Omega^* = \text{Re}(A)\sigma_x + \text{Im}(A)\sigma_y + C\sigma_z. \quad (\text{B12})$$

Due to the symmetry expressed by Eq. (B10), certain MC vanish, depending on the choice of P :

1. When $P = \sigma_z$, we have

$$P\Omega P = -\text{Re}(A)\sigma_x + \text{Im}(A)\sigma_y + C\sigma_z, \quad (\text{B13})$$

and thus $\text{Re}(A) = 0$, as we have seen in the discussion of LZSM model in Sec. III.

2. When $P = \sigma_x$, we have

$$P\Omega P = \text{Re}(A)\sigma_x + \text{Im}(A)\sigma_y - C\sigma_z, \quad (\text{B14})$$

leading to $C = 0$, as in region II for the Rabi model, discussed in Sec. IV.

3. When $f(-t) = f(t) \in \mathbb{R}$ in Eq. (1), the Hamiltonian displays time reflection symmetry, i.e., $H^*(-t) = H(t)$. Formally, this amounts to taking $P = \sigma_0$ in Eq. (B1), which results in $\text{Im}(A) = 0$. This symmetry, e.g., holds for $t \in [0, \pi/\omega]$, reflected about $t = \pi/2\omega$, if the shape function $\tilde{f}(t) = \sin \omega t$ is used in the Rabi model.

Appendix C: Exact and avoided crossings of quasienergy in two-level Floquet systems

In a periodically driven two-level system, due to the multi-valuedness of ϵ (which is defined modulo $\omega = 1$), quasienergy crossings can be grouped into two classes:

- 1) crossing in the middle of the BZ:

$$\epsilon = -\epsilon \Rightarrow \epsilon = 0 \Leftrightarrow U(2\pi) = \sigma_0$$

- 2) crossing of different branches (at the boundary of the BZ):

$$\epsilon = -\epsilon \pm 1 \Rightarrow \epsilon = \pm \frac{1}{2} \Leftrightarrow U(2\pi) = -\sigma_0$$

In both cases, any initial state reproduces itself after one period, up to a global phase factor. This provides a two-level interpretation of the coherent destruction of tunneling²¹, originally discovered in the periodically driven symmetric double-well potential model. In general, because an element in $SU(2)$ is characterized by three free parameters, realizing the crossing requires at least tuning three coupling constants in the Hamiltonian. This constitutes a particular case of the Wigner-von Neumann non-crossing rule⁷⁵. Crossings become much easier to achieve in the presence of symmetry, however, as explained below.

When $\tilde{f}(t)$ has the property $\tilde{f}(t + \pi) = -\tilde{f}(t)$, the Hamiltonian Eq. (1) displays the following adjoint symmetry

$$PH(t + \pi)P = H(t), \tag{C1}$$

where $P = \sigma_z$ in this case. More generally, we define Eq. (C1) as the generalized parity (GP) by allowing P to be a unitary Hermitian operator, satisfying

$$P^\dagger = P, \quad P^2 = \sigma_0, \quad \det P = -1. \tag{C2}$$

And thus P can be represented as

$$P = \vec{n}_P \cdot \vec{\sigma}, \quad |\vec{n}_P| = 1. \tag{C3}$$

With Eq. (C1) one may prove⁷⁹ that

$$U(2\pi) = [PU(\pi)]^2. \tag{C4}$$

Higher order Magnus expansions for two-level quantum dynamics

It follows from Eq. (C4) that $PU(\pi)$ has eigenvalues $\mp e^{\pm i\epsilon\pi}$ where ϵ is the quasienergy and its eigenstates are the initial Floquet states. Thus we have

$$\text{tr}[PU(\pi)] = -2i \sin(\epsilon\pi). \quad (\text{C5})$$

On the other hand, by writing $U(\pi)$ in angle-axis form $\exp(-i\theta\vec{n}\cdot\vec{\sigma})$, one finds

$$\text{tr}[PU(\pi)] = -2i(\vec{n}\cdot\vec{n}_P)\sin\theta. \quad (\text{C6})$$

Comparing the two equations above, one obtains

$$\sin(\epsilon\pi) = (\vec{n}\cdot\vec{n}_P)\sin\theta \quad (\text{C7})$$

Eq. (C7) explains explicitly the crossing and non-crossing rules of the quasienergies by the following argument. For case 1) to appear,

$$\sin\epsilon\pi = 0 \Leftrightarrow \theta = 0 \text{ or } \vec{n}\cdot\vec{n}_P = 0. \quad (\text{C8})$$

The set of allowed $U(\pi)$ thus is two-dimensional, and therefore it suffices to tune only one parameter to achieve an exact crossing at $\epsilon = 0$ in general. In contrast, case 2) is equivalent with

$$\sin\epsilon\pi = \pm 1 \Leftrightarrow \theta = \pm\frac{\pi}{2} \text{ and } \vec{n} = \pm\vec{n}_P, \quad (\text{C9})$$

that is, $\epsilon = \pm 1/2$ and $U(\pi) = \pm i\sqrt{P}$. This case is much harder to realize since the allowed set of $U(\pi)$ has zero measure in the $SU(2)$ group. Therefore under change of parameters, around $\epsilon = \pm 1/2$, i.e. at boundaries of the Brillouin zone, crossings are usually avoided.

REFERENCES

- ¹W. Magnus, “On the exponential solution of differential equations for a linear operator,” *Communications on Pure and Applied Mathematics* **7**, 649–673 (1954).
- ²L. D. Landau, “Zur Theorie der Energieübertragung. II,” *Physikalische Zeitschrift der Sowjetunion* **2**, 46–51 (1932).
- ³C. Zener, “Non-adiabatic crossing of energy levels,” *Proceedings of the Royal Society of London. Series A* **137**, 696–702 (1932).
- ⁴E. C. G. Stückelberg, “Theorie der inelastischen Stöße zwischen Atomen,” *Helvetica Physica Acta* **5**, 369–423 (1932).

- ⁵E. Majorana, “Teoria relativistica di particelle con spin arbitrario,” *Il Nuovo Cimento* **9**, 335–345 (1932).
- ⁶N. Rosen and C. Zener, “Double Stern-Gerlach Experiment and Related Collision Phenomena,” *Phys. Rev.* **40**, 502–507 (1932).
- ⁷I. I. Rabi, “On the process of space quantization,” *Phys. Rev.* **49**, 324–328 (1936).
- ⁸I. I. Rabi, “Space quantization in a gyrating magnetic field,” *Phys. Rev.* **51**, 652–654 (1937).
- ⁹F. Bloch and A. Siegert, “Magnetic Resonance for Nonrotating Fields,” *Phys. Rev.* **57**, 522–527 (1940).
- ¹⁰D. Braak, Q.-H. Chen, M. T. Batchelor, and E. Solano, “Semi-classical and quantum Rabi models: in celebration of 80 years,” *Journal of Physics A: Mathematical and Theoretical* **49**, 300301 (2016).
- ¹¹T. Ma and S.-M. Li, “Floquet system, Bloch oscillation, and Stark ladder,” (2007), arXiv:0711.1458 [cond-mat.other].
- ¹²Q. Xie and W. Hai, “Analytical results for a monochromatically driven two-level system,” *Phys. Rev. A* **82**, 032117 (2010).
- ¹³C. Wittig, “The Landau-Zener formula,” *The Journal of Physical Chemistry B* **109**, 8428–8430 (2005).
- ¹⁴A. C. Vutha, “A simple approach to the Landau-Zener formula,” *European Journal of Physics* **31**, 389 (2010).
- ¹⁵L. T. A. Ho and L. F. Chibotaru, “A simple derivation of the Landau-Zener formula,” *Phys. Chem. Chem. Phys.* **16**, 6942–6945 (2014).
- ¹⁶E. P. Glasbrenner and W. P. Schleich, “The Landau-Zener formula made simple,” *Journal of Physics B: Atomic, Molecular and Optical Physics* **56**, 105001 (2023).
- ¹⁷E. P. Glasbrenner, Y. Gerdes, S. Varró, and W. P. Schleich, “Riccati equation perspective on Landau-Zener transitions,” *Phys. Rev. Res.* **7**, 043208 (2025).
- ¹⁸C. Sun, “Derivation of the Landau-Zener formula via functional equations,” *Journal of Physics A: Mathematical and Theoretical* **58**, 37LT01 (2025).
- ¹⁹J. C. Tully and R. K. Preston, “Trajectory Surface Hopping Approach to Nonadiabatic Molecular Collisions: The Reaction of H⁺ with D₂,” *The Journal of Chemical Physics* **55**, 562–572 (1971).
- ²⁰N. Cindro, R. M. Freeman, and F. Haas, “Experimental evidence and the Landau-Zener

- promotion in nucleus-nucleus collisions,” *Phys. Rev. C* **33**, 1280–1287 (1986).
- ²¹F. Großmann, T. Dittrich, P. Jung, and P. Hänggi, “Coherent destruction of tunneling,” *Phys. Rev. Lett.* **67**, 516–519 (1991).
- ²²F. Großmann and P. Hänggi, “Localization in a driven two-level dynamics,” *Europhysics Letters* **18**, 571 (1992).
- ²³J. M. Gomez Llorente and J. Plata, “Tunneling control in a two-level system,” *Phys. Rev. A* **45**, R6958–R6961 (1992).
- ²⁴L. Wang and J. Shao, “Localization of two-level systems,” *Phys. Rev. A* **49**, R637–R640 (1994).
- ²⁵Y. Kayanuma, “Role of phase coherence in the transition dynamics of a periodically driven two-level system,” *Phys. Rev. A* **50**, 843–845 (1994).
- ²⁶M. Grifoni and P. Hänggi, “Driven quantum tunneling,” *Physics Reports* **304**, 229–354 (1998).
- ²⁷Y. Kayanuma and K. Saito, “Coherent destruction of tunneling, dynamic localization, and the Landau-Zener formula,” *Phys. Rev. A* **77**, 010101 (2008).
- ²⁸J. Cao, C. J. Bardeen, and K. R. Wilson, “Molecular π pulses: Population inversion with positively chirped short pulses,” *The Journal of Chemical Physics* **113**, 1898–1909 (2000).
- ²⁹K. Saito, M. Wubs, S. Kohler, P. Hänggi, and Y. Kayanuma, “Quantum state preparation in circuit QED via Landau-Zener tunneling,” *Europhysics Letters* **76**, 22 (2006).
- ³⁰H. Ribeiro and G. Burkard, “Nuclear State Preparation via Landau-Zener-Stückelberg Transitions in Double Quantum Dots,” *Phys. Rev. Lett.* **102**, 216802 (2009).
- ³¹L. Van Damme, Q. Ansel, S. J. Glaser, and D. Sugny, “Robust optimal control of two-level quantum systems,” *Phys. Rev. A* **95**, 063403 (2017).
- ³²A. Gangopadhyay, M. Dzero, and V. Galitski, “Exact solution for quantum dynamics of a periodically driven two-level system,” *Phys. Rev. B* **82**, 024303 (2010).
- ³³E. Barnes and S. Das Sarma, “Analytically Solvable Driven Time-Dependent Two-Level Quantum Systems,” *Phys. Rev. Lett.* **109**, 060401 (2012).
- ³⁴P. R. Berman, L. Yan, K.-H. Chiam, and R. Sung, “Nonadiabatic transitions in a two-level quantum system: Pulse-shape dependence of the transition probability for a two-level atom driven by a pulsed radiation field,” *Phys. Rev. A* **57**, 79–92 (1998).
- ³⁵C. W. S. Conover, “Effects of pulse shape on strongly driven two-level systems,” *Phys. Rev. A* **84**, 063416 (2011).

- ³⁶M. F. Linder, C. Schneider, J. Sickling, N. Szpak, and R. Schützhold, “Pulse shape dependence in the dynamically assisted Sauter-Schwinger effect,” *Phys. Rev. D* **92**, 085009 (2015).
- ³⁷J. P. Davis and P. Pechukas, “Nonadiabatic transitions induced by a time-dependent Hamiltonian in the semiclassical/adiabatic limit: The two-state case,” *The Journal of Chemical Physics* **64**, 3129–3137 (1976).
- ³⁸M. V. Berry, “Histories of adiabatic quantum transitions,” *Proceedings of the Royal Society of London. A. Mathematical and Physical Sciences* **429**, 61–72 (1990).
- ³⁹T. Matsuda, “Exact WKB analysis for dynamical and geometric exponents in generalized and nonlinear Landau-Zener transitions,” *Phys. Rev. A* **112**, 032224 (2025).
- ⁴⁰F. Großmann, *Theoretical Femtosecond Physics: Atoms and Molecules in Strong Laser Fields*, 3rd ed., Graduate Texts in Physics (Springer International Publishing, Cham, Switzerland, 2018).
- ⁴¹P. W. Langhoff, S. T. Epstein, and M. Karplus, “Aspects of Time-Dependent Perturbation Theory,” *Rev. Mod. Phys.* **44**, 602–644 (1972).
- ⁴²S. Blanes, F. Casas, J. Oteo, and J. Ros, “The Magnus expansion and some of its applications,” *Physics Reports* **470**, 151–238 (2009).
- ⁴³A. López, A. Scholz, Z. Sun, and J. Schliemann, “Graphene with time-dependent spin-orbit coupling: truncated Magnus expansion approach,” *The European Physical Journal B* **86**, 366 (2013).
- ⁴⁴U. Haeberlen and J. S. Waugh, “Coherent Averaging Effects in Magnetic Resonance,” *Phys. Rev.* **175**, 453–467 (1968).
- ⁴⁵W. Evans, “On some applications of the Magnus expansion in nuclear magnetic resonance,” *Annals of Physics* **48**, 72–93 (1968).
- ⁴⁶E. Fel’dman, “On the convergence of the Magnus expansion for spin systems in periodic magnetic fields,” *Physics Letters A* **104**, 479–481 (1984).
- ⁴⁷P. Nalbach and V. Leyton, “Magnus expansion for a chirped quantum two-level system,” *Phys. Rev. A* **98**, 023855 (2018).
- ⁴⁸T. K. Begzjav and H. Eleuch, “Magnus expansion applied to a dissipative driven two-level system,” *Results in Physics* **17**, 103098 (2020).
- ⁴⁹M. Klaiber, D. Dimitrovski, and J. Briggs, “The Magnus expansion for interaction of atoms with attosecond laser pulses,” *Journal of Physics B: Atomic, Molecular and Optical*

- Physics **41** (2008).
- ⁵⁰P. Pechukas and J. C. Light, “On the Exponential Form of Time-Displacement Operators in Quantum Mechanics,” *The Journal of Chemical Physics* **44**, 3897–3912 (1966).
- ⁵¹W. Salzman, “On the convergence of exponential perturbation theories in the Schrödinger representation,” *Chemical Physics Letters* **124**, 531–533 (1986).
- ⁵²M. M. Maricq, “Convergence of the Magnus expansion for time dependent two level systems,” *The Journal of Chemical Physics* **86**, 5647–5651 (1987).
- ⁵³V. Jakubovič and V. Staržinskij, *Linear Differential Equations with Periodic Coefficients*, A Halsted Press book (Wiley, 1975).
- ⁵⁴S. Blanes, F. Casas, J. A. Oteo, and J. Ros, “Magnus and Fer expansions for matrix differential equations: the convergence problem,” *Journal of Physics A: Mathematical and General* **31**, 259 (1998).
- ⁵⁵F. Casas, “Sufficient conditions for the convergence of the Magnus expansion,” *Journal of Physics A: Mathematical and Theoretical* **40**, 15001 (2007).
- ⁵⁶W. R. Salzman, “Convergence of Magnus and Magnus-like expansions in the Schrödinger representation,” *The Journal of Chemical Physics* **85**, 4605–4613 (1986).
- ⁵⁷M. Born and V. Fock, “Beweis des Adiabatsatzes,” *Zeitschrift für Physik* **51**, 165–180 (1928).
- ⁵⁸B. C. Hall, *Lie Groups, Lie Algebras, and Representations: An Elementary Introduction*, Graduate Texts in Mathematics, Vol. 222 (Springer Cham, 2015) 2nd edition.
- ⁵⁹A. Alvermann and H. Fehske, “High-order commutator-free exponential time-propagation of driven quantum systems,” *Journal of Computational Physics* **230**, 5930–5956 (2011).
- ⁶⁰D. J. Tannor, *Introduction to quantum mechanics : a time-dependent perspective* (Univ. Science Books, 2007).
- ⁶¹L. M. Garrido, “Generalized Adiabatic Invariance,” *Journal of Mathematical Physics* **5**, 355–362 (1964).
- ⁶²M. V. Berry, “Quantum phase corrections from adiabatic iteration,” *Proceedings of the Royal Society of London. A. Mathematical and Physical Sciences* **414**, 31–46 (1987).
- ⁶³S. Klarsfeld and J. A. Oteo, “Magnus approximation in the adiabatic picture,” *Phys. Rev. A* **45**, 3329–3332 (1992).
- ⁶⁴S. Stenholm, “Simple quantum dynamics,” in *Quantum Dynamics of Simple Systems*, edited by G. L. Oppo, S. M. Barnett, E. Riis, and M. Wilkinson (IOP, Bristol, 1996) p.

267.

- ⁶⁵M. V. Berry, “Quantal phase factors accompanying adiabatic changes,” *Proceedings of the Royal Society of London. A. Mathematical and Physical Sciences* **392**, 45–57 (1984).
- ⁶⁶Y. Kayanuma, “Stokes phase and geometrical phase in a driven two-level system,” *Phys. Rev. A* **55**, R2495–R2498 (1997).
- ⁶⁷S. Shevchenko, S. Ashhab, and F. Nori, “Landau-Zener-Stückelberg interferometry,” *Physics Reports* **492**, 1–30 (2010).
- ⁶⁸F. Forster, G. Petersen, S. Manus, P. Hänggi, D. Schuh, W. Wegscheider, S. Kohler, and S. Ludwig, “Characterization of Qubit Dephasing by Landau-Zener-Stückelberg-Majorana Interferometry,” *Phys. Rev. Lett.* **112**, 116803 (2014).
- ⁶⁹A. M. Dykhne, “Adiabatic perturbation of discrete spectrum states,” *Soviet Physics JETP* **14**, 941–943 (1962).
- ⁷⁰J. H. Shirley, “Solution of the Schrödinger Equation with a Hamiltonian Periodic in Time,” *Phys. Rev.* **138**, B979–B987 (1965).
- ⁷¹D. Zeuch, F. Hassler, J. J. Slim, and D. P. DiVincenzo, “Exact rotating wave approximation,” *Annals of Physics* **423**, 168327 (2020).
- ⁷²R. Gilmore, “Baker-Campbell-Hausdorff formulas,” *Journal of Mathematical Physics* **15**, 2090–2092 (1974).
- ⁷³P. M. Schindler and M. Bukov, “Geometric Floquet Theory,” *Phys. Rev. X* **15**, 031037 (2025).
- ⁷⁴F. Großmann, P. Jung, T. Dittrich, and P. Hänggi, “Tunneling in a Periodically Driven Bistable System,” *Zeitschrift für Physik B* **84**, 315 (1991).
- ⁷⁵J. von Neumann and E. P. Wigner, “Über das Verhalten von Eigenwerten bei adiabatischen Prozessen,” in *The Collected Works of Eugene Paul Wigner: Part A: The Scientific Papers* (Springer Berlin Heidelberg, Berlin, Heidelberg, 1993) pp. 294–297.
- ⁷⁶F. Großmann, *Der Tunneleffekt in periodisch getriebenen Quantensystemen*, Ph.D. thesis, Universität Augsburg (1992).
- ⁷⁷C. Creffield, “Location of crossings in the Floquet spectrum of a driven two-level system,” *Phys. Rev. B* **67**, 165301 (2003).
- ⁷⁸H.-J. Schmidt, “The Floquet Theory of the Two-Level System Revisited,” *Zeitschrift für Naturforschung A* **73**, 705–731 (2018).
- ⁷⁹H.-J. Schmidt, J. Schnack, and M. Holthaus, “Floquet theory of the analytical solution of

- a periodically driven two-level system,” *Applicable Analysis* **100**, 992 (2021).
- ⁸⁰DLMF, “*NIST Digital Library of Mathematical Functions*,” <https://dlmf.nist.gov/>, Release 1.2.4 of 2025-03-15, f. W. J. Olver, A. B. Olde Daalhuis, D. W. Lozier, B. I. Schneider, R. F. Boisvert, C. W. Clark, B. R. Miller, B. V. Saunders, H. S. Cohl, and M. A. McClain, eds.
- ⁸¹M. Abramowitz and I. Stegun, *Handbook of mathematical functions with formulas, graphs, and mathematical tables* (Dover, New York, 1964).
- ⁸²C. E. Creffield and G. Sierra, “Finding zeros of the Riemann zeta function by periodic driving of cold atoms,” *Phys. Rev. A* **91**, 063608 (2015).
- ⁸³A. Dey, D. Lonigro, K. Yuasa, and D. Burgarth, “Error bounds for the Floquet-Magnus expansion and their application to the semiclassical quantum Rabi model,” *Phys. Rev. A* **112**, 053723 (2025).
- ⁸⁴M. Wagner and P. Vasilopoulos, “Dynamics of strongly driven two-level systems: analytical solutions,” *Superlattices and Microstructures* **23**, 477–483 (1998).
- ⁸⁵Y. Liu, L. Duan, and Q.-H. Chen, “Analytical study of the non-Hermitian semiclassical Rabi model,” *Phys. Rev. Res.* **7**, 023004 (2025).
- ⁸⁶M. Byrd, “Differential geometry on $SU(3)$ with applications to three state systems,” *Journal of Mathematical Physics* **39**, 6125–6136 (1998).
- ⁸⁷G. Lakos, “Convergence estimates for the Magnus expansion IIA. 2×2 matrices with operator norm,” arXiv preprint (2023), arXiv:2304.03513, arXiv:2304.03513 [math.SP].
- ⁸⁸F. Petiziol, F. Mintert, and S. Wimberger, “Quantum control by effective counterdiabatic driving,” *Europhysics Letters* **145**, 15001 (2024).
- ⁸⁹M. V. Berry, “Transitionless quantum driving,” *Journal of Physics A: Mathematical and Theoretical* **42**, 365303 (2009).
- ⁹⁰S. Klarsfeld and J. A. Oteo, “Recursive generation of higher-order terms in the Magnus expansion,” *Phys. Rev. A* **39**, 3270–3273 (1989).